

Drift 1000 1/2
2612

JOINT INSTITUTE FOR ADVANCEMENT OF FLIGHT SCIENCES

✓ A RESEARCH PROGRAM IN ACTIVE CONTROL/AEROELASTICITY

NASA GRANT NAG1-199

(NASA-CR-176773) A RESEARCH PROGRAM IN N86-24702
ACTIVE CONTROL/AEROELASTICITY Final
Semiannual Status Report, May - Oct. 1985
(Georgetown Univ., Washington, D.C.) 15 p Unclass
HC A02/MF A01 CSCL 01C G3/08 43383

Final Semi-Annual Status Report

May 1985 - October 1985

School of Engineering and Applied Science
The George Washington University
Washington, D. C. 20052

GV 900286

The program objectives are fully defined in the original proposal entitled "A Research Program in Active Control/Aeroelasticity in the JIAFS at the NASA Langley Research Center" dated August 1, 1981.

The research conducted by Dr. V. Mukhopadhyay during this report period and a summary of the overall research activities are described below:

Development of Synthesis Methodology for Multifunctional Robust Aeroservoelastic System

Introduction

A synthesis methodology for multifunctional robust aeroservoelastic systems was developed. The development consisted of the following stages:

1. Development of an universal diagram to determine phase and gain margins of a multi-input multi-output (MIMO) system using singular value based stability margin criteria.
2. Determination of singular value gradients with respect to design parameters and their application to improve stability margins of multiloop system.
3. Application of constrained optimization techniques to synthesize a low order robust controller for a high order MIMO aeroservoelastic system while satisfying several design constraints on the dynamic loads and responses and stability margins at the plant input and output.

System Description

The MIMO feedback control system is described by the block diagram shown in Figure 1. The plant has several inputs and outputs denoted by vector U and Y' respectively. The root-mean square (RMS) dynamic loads and responses on which

upper-bound constraints may be applied are denoted by vector Y_D . The maximum allowable value vector in $Y_{D\text{MAX}}$. The plant state-space matrices F , G_u , H and an initial dynamic controller state-space matrices A , B , C are given. The initial controller may be obtained using Linear quadratic Gaussian (LQG) methodology, controller order reduction techniques or from a previous classical design. The initial closed-loop system must be stable. The expressions $G(s)$ and $K(s)$ represent the plant and the controller transfer function matrices respectively, in the Laplace domain. The matrices R_U and P_V are so-called fictitious plant and measurement noise intensity matrices which can be used to improve the stability margins at the plant input (denoted by point (1)) and plant output (denoted by point (2)) for a full order LQG controller design.

In order to maintain certain phase and gain margins at the points (1) and/or (2) one must satisfy the conditions

$$\underline{\sigma}(I+KG) > \underline{\sigma}_{D1}(\omega) \quad \text{at input} \quad (1)$$

$$\underline{\sigma}(I+GK) > \underline{\sigma}_{D2}(\omega) \quad \text{at output} \quad (2)$$

where $\underline{\sigma}$ denotes minimum singular value and is a measure of lower bound of the matrices in the parenthesis over the entire frequency range $0 \leq \omega < \infty$.

The inequalities (1) and (2) can be directly related to the desired phase and gain margins of a MIMO system using the universal diagram shown in Figure 2. Note that the singular value based stability margin criteria are sufficient conditions and may be conservative in nature.

Problem Definition

The controller synthesis scheme is posed as a constrained optimization problem in an LQG framework and is shown in Figure 3. The cost function is a weighted sum of the expected value of steady state RMS plant outputs and controller

outputs. The constraints g_1 and g_2 are scalars and are a cumulative measure of the difference between desired singular value shape and actual minimum singular value spectrum. The vector g_3 represents all dynamic loads and design response constraints. The optimization algorithm uses the method of feasible directions to reduce all the constraints to zero or negative while minimizing the objective function J .

Optimization Scheme

The optimization scheme block diagram is shown in Figure 4. Starting from an initial stabilizing controller, the closed loop system matrices are computed. A set of Lyapunov equations are solved to obtain the objective function, the response constraints and their gradients with respect to the design variables. The singular values and their gradients are also obtained from analytical expressions. This information is used to update the controller using the method of feasible directions. The optimization algorithm CONMIN first attempts to satisfy all constraints while minimizing the objective function.

Example Problem

The synthesis method was applied to a two-input two-output system which represents a drone aircraft with a lateral attitude control system. A block diagram of the system is shown in Figure 5. The plant input position 1 is defined at the entry point to the elevon and rudder actuators denoted by U_1 and U_2 in degrees units. The plant output position 2 is defined at the roll rate and yaw rate sensor outputs denoted by Y_1 and Y_2 in degrees/second unit. The noise intensity matrices R_U and R_Y can be used to improve the stability margins for the full order LQG controller. This is demonstrated in Figures 6 and 7 and Design Nos. 1 to 5 and are tabulated in Table I. In Design No. 1, for large value of

R_V , the plant is made robust at plant output but not at plant input as indicated by the singular value plots in Figure 6. By increasing R_U as compared to R_V , the situation is gradually reversed as indicated by the Design Nos. 2, 3 and 4, in Figures 6 and 7. The singular value plot in Design No. 5 shows the beneficial effects of imposing more uncertainty in the unstable rudder channel. This design is used as a starting point for testing the present constrained optimization design procedure, to improve stability margins at both the plant input and output. In these designs the weighting matrices $Q_1 = I$ and $Q_2 = 0.5I$ where I is appropriate identity matrix. The contributions of U' and Y' to the objective function J are roughly equal. The noise intensity matrices R_U and R_V are set to zero. The system only contains a unit RMS white noise at the elevon actuator input. All the elements of matrices B and C are design variables and matrix $A = (F + G_U C - BH)$ as in a Kalman Filter. The minimum desired singular value $\underline{\sigma}_D = 0.45$ is chosen as constraints on both $\underline{\sigma}(I + KG)$ and $\underline{\sigma}(I + GK)$ at the plant input and outputs respectively. In computing the cumulative constraints, the frequency points are chosen uniformly in log scale as 50 divisions per decade. The Design No. 6, in Figure 7 shows the singular value spectrum after five iterations. The minimum $\underline{\sigma}(I + KG)$ and $\underline{\sigma}(I + GK)$ are increased from 0.33 and 0.25 to 0.4 and 0.38 respectively. Thus the present constrained optimization procedure is able to improve the stability robustness at both input and output. However, the improvement is at the cost of some loss of high frequency attenuation at the plant input. The Design Nos. 7, 8 and 9 in Table I and Figure 8 show additional results for a third order controller using truncation, and optimization methods with the two types of constraints (A and B, as shown in Figure 3).

Concise Statement of Research Accomplished

A design methodology for multi-functional robust feedback controller was

developed. The method used constrained optimization techniques to improve stability margins of a multiloop system at both the plant input and output, while minimizing a standard LQC performance index. The method can also be used to impose additional constraints on steady state and PMS responses.

Publications

1. Mukhopadhyay, V., "Constrained Optimization Techniques for Active Control of Aeroelastic Response," Paper presented at the Symposium on Recent Trends in Aeroelasticity, Structures and Structural Dynamics, Gainesville, Florida, February 6-7, 1986.
2. Mukhopadhyay, V., "Stability Robustness Improvement Using Constrained Optimization Technique," AIAA Paper No. 85-1931, presented at AIAA Guidance & Control Conference, August 19-21, 1985, Snowmass, Colorado.
3. Newsom, J. R., and Mukhopadhyay, V., "A Multiloop Robust Controller Design Study Using Singular Value Gradients," Journal of Guidance Control and Dynamics, Vol. 8, No. 4, July-August 1985, pp. 514-519.
4. Mukhopadhyay, V., and Newsom, J. R., "A Multi-loop System Stability Margin Study Using Matrix Singular Values," Journal of Guidance Control and Dynamics, Vol. 7, No. 5, Sept.-Oct. 1984, pp. 582-587.
5. Newsom, J. R., and Mukhopadhyay, V., "The Use of Singular Value Gradients and Optimization Techniques to Design Robust Controller for Multiloop Systems," AIAA Paper No. 83-2191, presented at AIAA Guidance and Control Conference, Gatlinberg, Tennessee, August 15-17, 1983.
6. Mukhopadhyay, V., and Newsom, J.R., "Application of Matrix Singular Value Properties for Evaluating Gain and Phase Margins of Multiloop Systems," AIAA Paper No. 82-1574, presented at AIAA Guidance and Control Conference, San Diego, California, August 9-11, 1982. (Also NASA Technical Memo. No. NASA TM-84524, August 1982).
7. Newsom, J. R., Adams, W. M., Mukhopadhyay, V., Abel, I., and Tiffany, S. H., "Active Controls: A Look at Analytical Methods and Associated Tools," Proceedings of the 14th Congress of the International Council of Aeronautical Sciences, Toulouse, France, September 10-14, 1984, ICAS-84-4.2.3. (Also AIAA Paper No. 84-1054, presented at AIAA Dynamics Specialists Conference, Palm Springs, California, May 17-18, 1984).

Table - 1 Summary of Design Parameters and RMS Responses

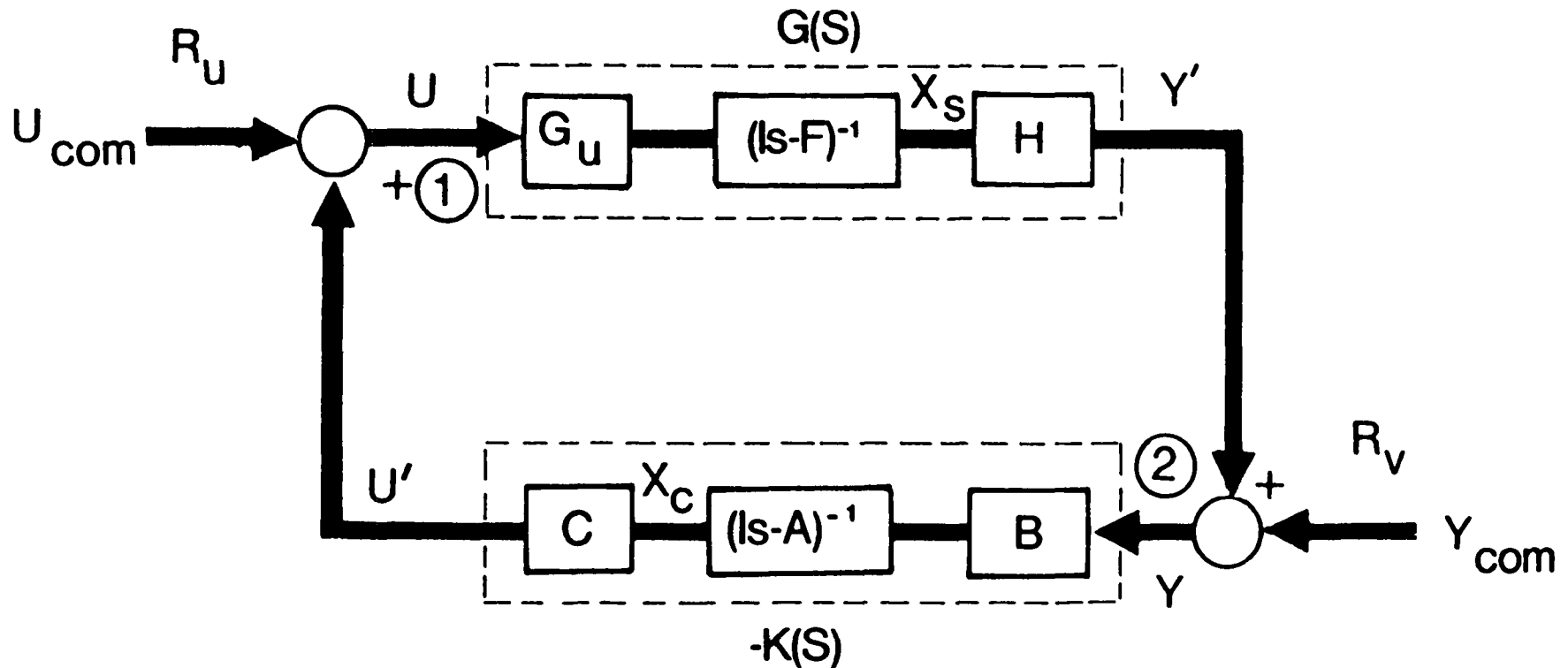
Design No.	Input Noise Intensity R_u	Sensor Noise Intensity R_v	Order of Controller	Design Procedure*	$\sigma_{\min} (I+KG)$	$\sigma_{\min} (I+GK)$	RMS RESPONSE TO UNIT RMS NOISE AT U_1				
							Side Slip β	Roll Rate $\dot{\phi}$	Yaw Rate $\dot{\psi}$	Elevon Defl. δ_1	Rudder Defl. δ_2
1	I	100I	6	LQG	0.15	0.83	0.27	2.69	0.59	3.37	0.36
2	I	I	6	LQG	0.20	0.50	0.11	1.68	0.21	3.43	0.25
3	I	0.01I	6	LQG	0.53	0.10	0.11	1.30	0.24	3.26	0.59
4	1000I	I	6	LQG	0.68	0.05	0.09	1.19	0.21	3.14	0.53
5	$\begin{bmatrix} 1 \\ 0 \\ 100 \end{bmatrix}$	$\begin{bmatrix} 1 \\ 0 \\ 10 \end{bmatrix}$	6	LQG	0.33	0.25	0.07	1.24	0.20	3.24	0.45
6	$\begin{bmatrix} 0 \\ 0 \\ 0 \end{bmatrix}$	$\begin{bmatrix} 0 \\ 0 \\ 0 \end{bmatrix}$	6	O(A)	0.40	0.38	0.02	1.27	0.13	3.31	0.22
7	$\begin{bmatrix} 0 \\ 0 \\ 0 \end{bmatrix}$	$\begin{bmatrix} 0 \\ 0 \\ 0 \end{bmatrix}$	3	T	0.17	0.10	0.16	1.56	0.19	3.26	0.36
8	$\begin{bmatrix} 0 \\ 0 \\ 0 \end{bmatrix}$	$\begin{bmatrix} 0 \\ 0 \\ 0 \end{bmatrix}$	3	O(A)	0.22	0.40	0.03	1.48	0.14	3.59	0.71
9	$\begin{bmatrix} 0 \\ 0 \\ 0 \end{bmatrix}$	$\begin{bmatrix} 0 \\ 0 \\ 0 \end{bmatrix}$	3	O(B)	0.26	0.22	0.08	1.46	0.14	3.25	0.12

* O(A) - Optimization (Type A Constraint)

O(B) - Optimization (Type B Constraint)

T - Truncation of Design No. 6

FIG.1 . **SYSTEM DESCRIPTION**



Need

$$\left. \begin{array}{l} \textcircled{1} \quad \underline{\sigma}(I + KG) \geq \underline{\sigma}_{D1}(\omega) \\ \textcircled{2} \quad \underline{\sigma}(I + GK) \geq \underline{\sigma}_{D2}(\omega) \end{array} \right\} \text{Stability Robustness}$$

Also

$$Y_D \leq Y_{D\text{MAX}} \quad (\text{RMS}) \quad \text{Dynamic Load and Responses}$$

FIG.2 UNIVERSAL DIAGRAM FOR GAIN PHASE MARGIN EVALUATION

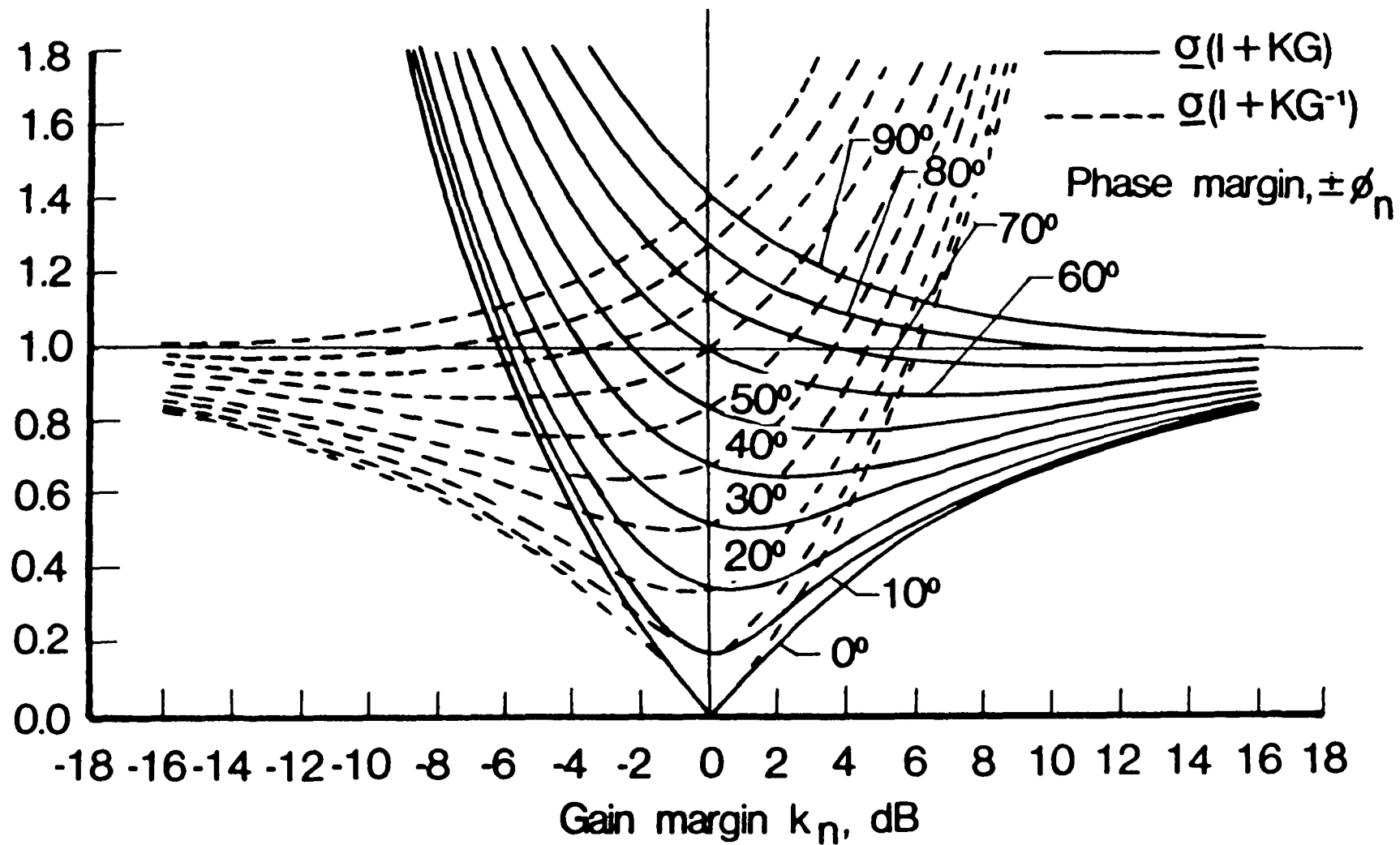


FIG. 3

PROBLEM DEFINITION

Minimize $J = E (Y'^T Q_1 Y' + U'^T Q_2 U')_{ss}$

Subject to

At input $g_1 = \frac{1}{N} \sum_{n=1}^N \max \left[0, \{ \underline{\sigma}_{D1} - \underline{\sigma} (I + KG) \}_n \right] \leq 0$

At output $g_2 = \frac{1}{N} \sum_{n=1}^N \max \left[0, \{ \underline{\sigma}_{D2} - \underline{\sigma} (I + GK) \}_n \right] \leq 0$

also $g_3 = E (Y_D / \bar{Y}_{D\text{MAX}})^2 - 1 \leq 0$

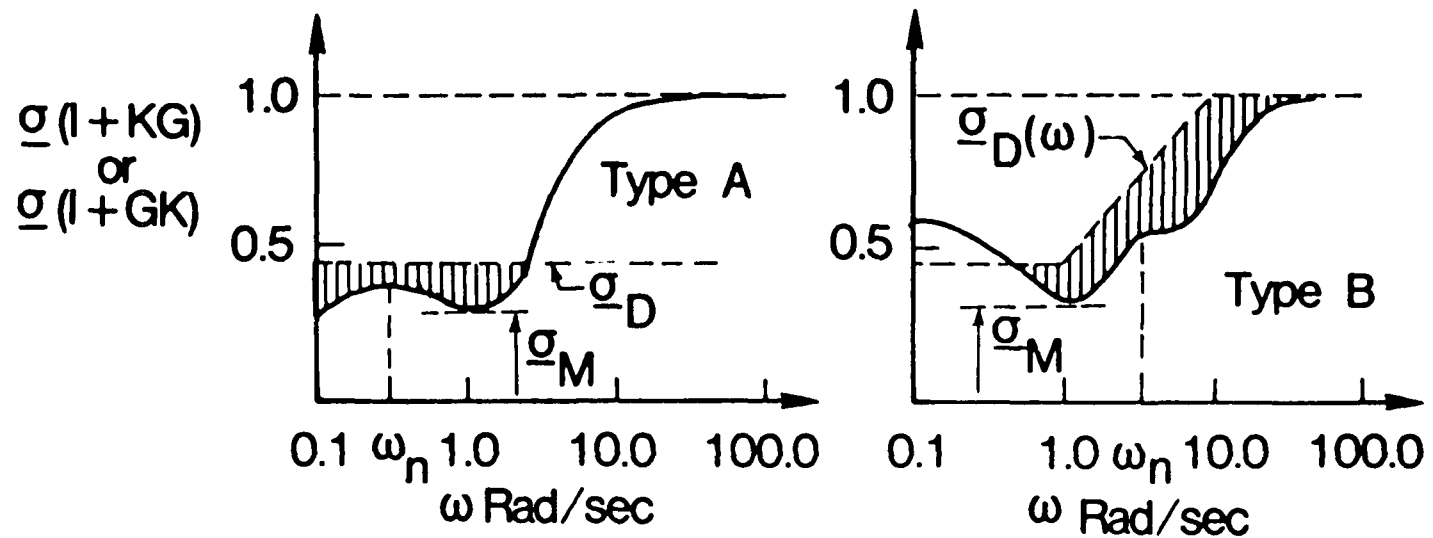


FIG.4 OPTIMIZATION SCHEME BLOCK DIAGRAM

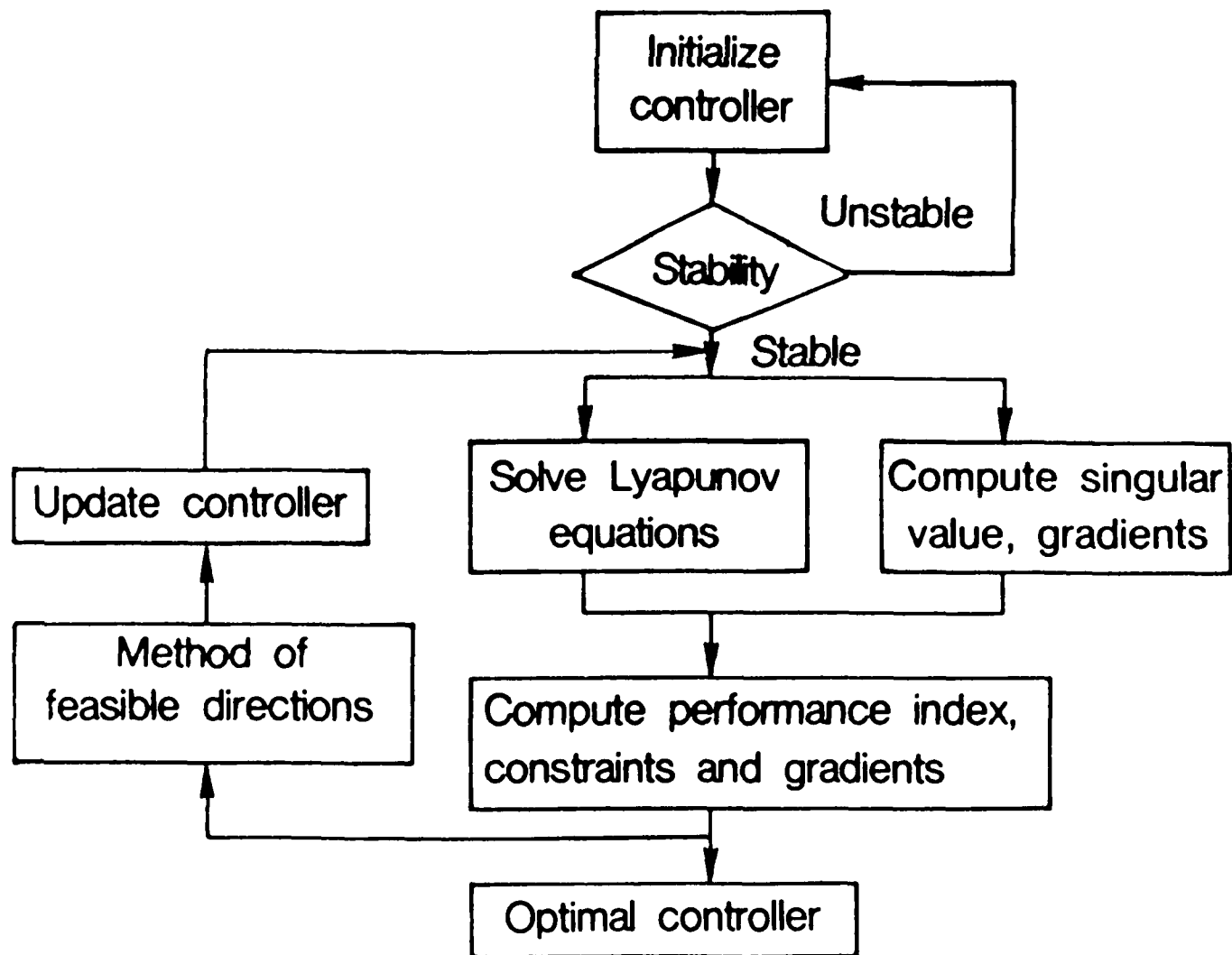
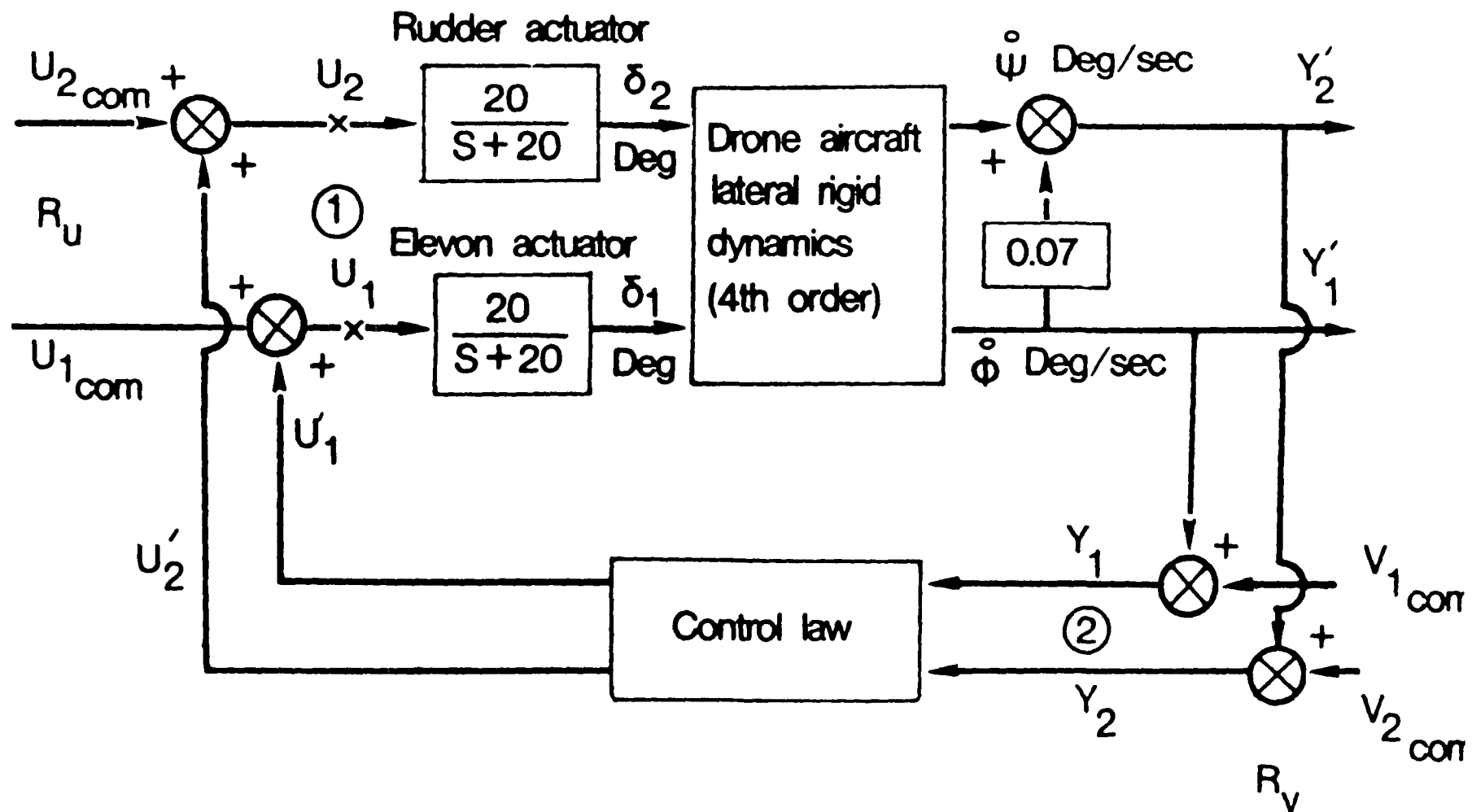
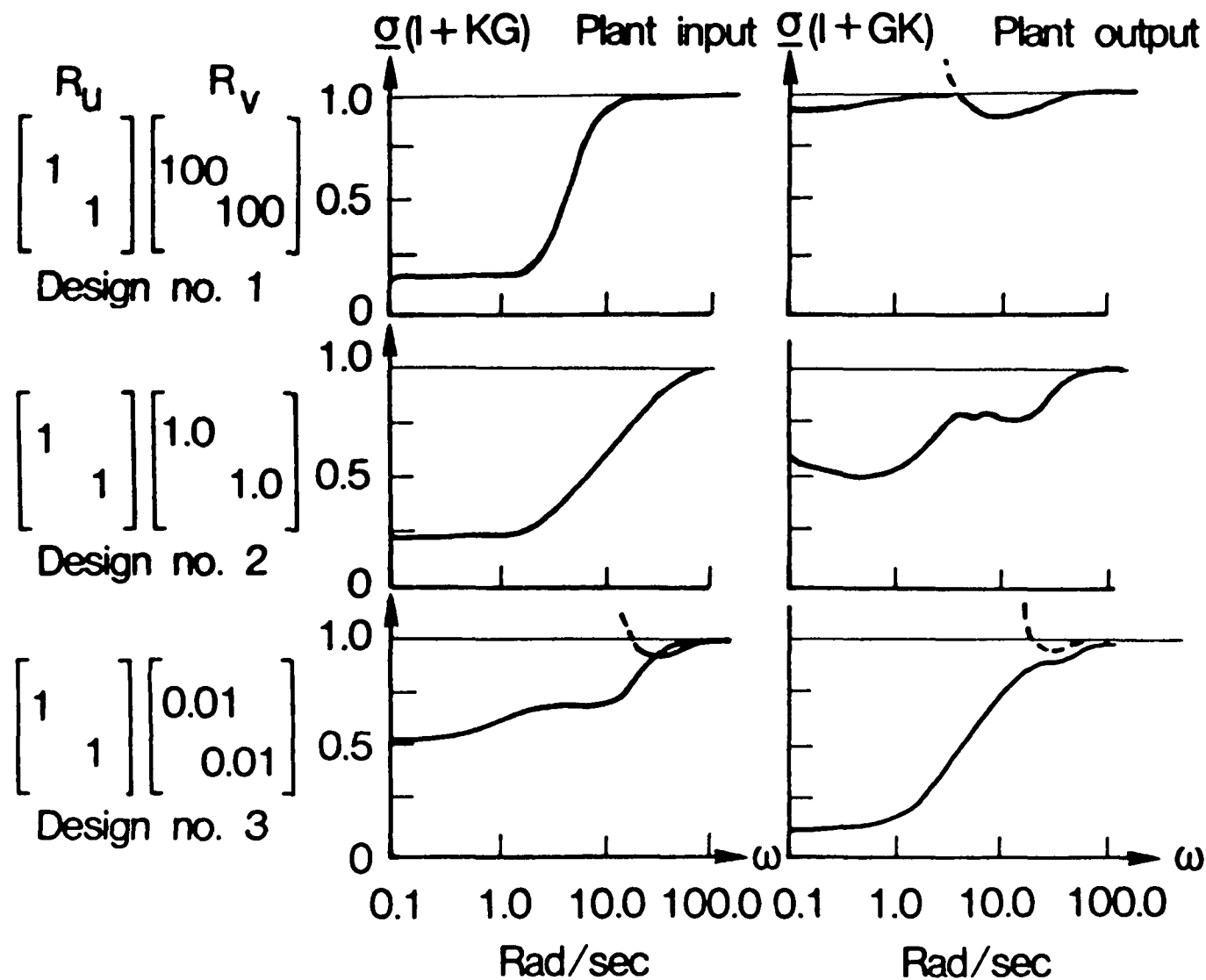


FIG.5 . EXAMPLE PROBLEM BLOCK DIAGRAM



**FIG. 6 SINGULAR VALUE SHAPING
BY NOISE ADJUSTMENT — FULL ORDER CONTROLLER**



**FIG.7 SINGULAR VALUE SHAPING BY NOISE ADJUSTMENT
AND CONSTRAINED OPTIMIZATION — FULL ORDER
CONTROLLER**

$$R_u = \begin{bmatrix} 1000 \\ 1000 \end{bmatrix} \quad R_v = \begin{bmatrix} 1 \\ 1 \end{bmatrix}$$

Design no. 4

$$\begin{bmatrix} 1 \\ 100 \end{bmatrix} \quad \begin{bmatrix} 1 \\ 10 \end{bmatrix}$$

Design no. 5

(Constrained
optimization of
design 5)

Design no. 6

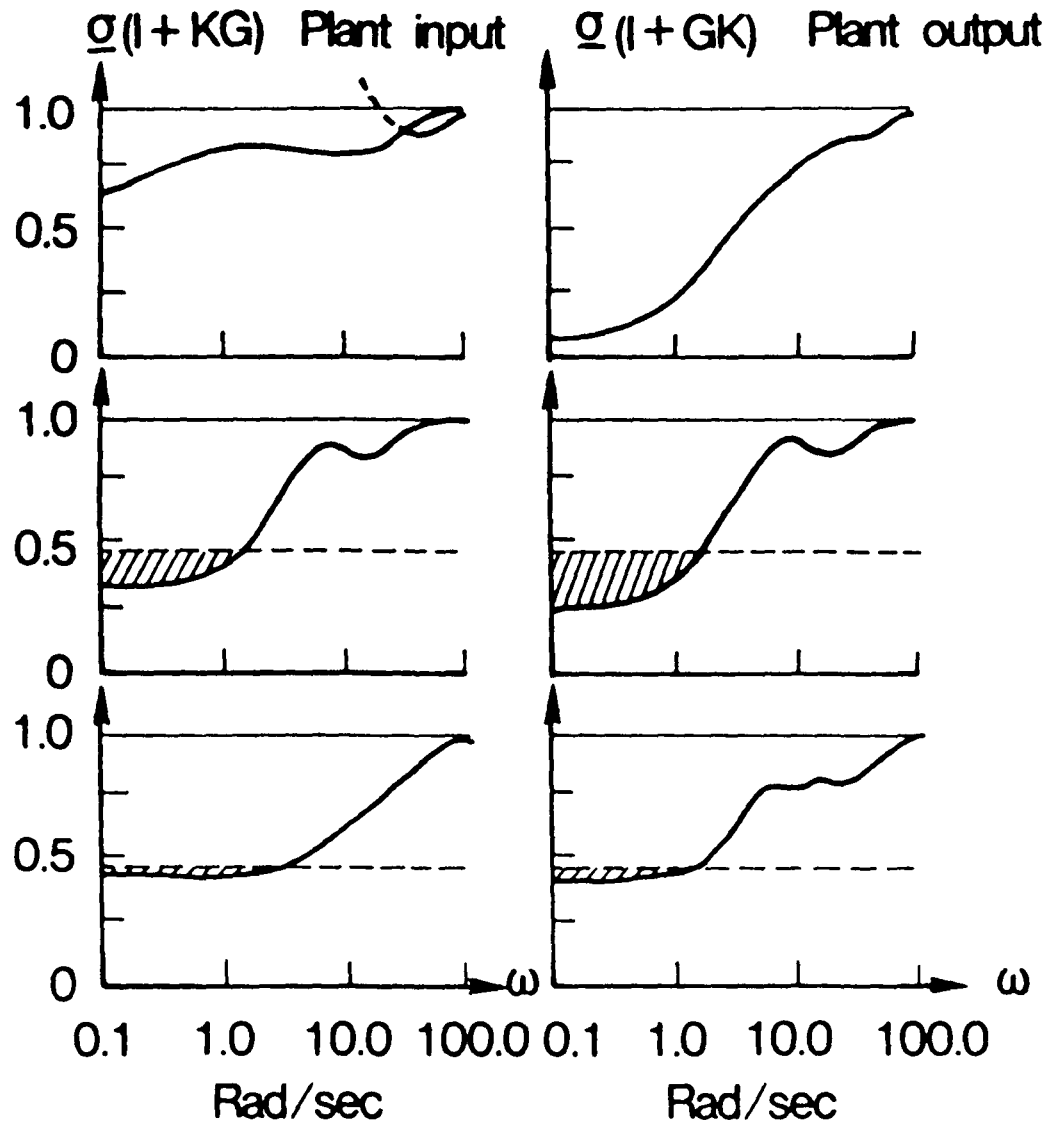


FIG.8 SINGULAR VALUE SHAPING BY CONSTRAINED OPTIMIZATION — 3RD ORDER CONTROLLER

